scientific reports

Check for updates

OPEN

Analysis of abiotic and biotic stress-induced Ca^{2+} transients in the crop species *Solanum tuberosum*

Annelotte van Dieren[1]✉, Roland E. Schwarzenbacher[2], Sophia Sonnewald[3], Andras Bittner[1] & Ute C. Vothknecht[1]✉

Secondary messengers, such as calcium ions (Ca^{2+}), are integral parts of a system that transduces environmental stimuli into appropriate cellular responses. Different abiotic and biotic stresses as well as developmental processes trigger temporal increases in cytosolic free Ca^{2+} levels by an influx from external and internal stores. Stimulus-specificity is obtained by a certain amplitude, duration, oscillation and localisation of the response. Most knowledge on stress-specific Ca^{2+} transient, called calcium signatures, has been gained in the model plant *Arabidopsis thaliana*, while reports about stress-related Ca^{2+} signalling in crop plants are comparatively scarce. In this study, we introduced the Ca^{2+} biosensor apoaequorin into potato (*Solanum tuberosum*, Lcv. Désirée). We observed dose-dependent calcium signatures in response to a series of stress stimuli, including H_2O_2, NaCl, mannitol and pathogen-associated molecular patterns (PAMPs) with stimuli-specific kinetics. Direct comparison with Arabidopsis revealed differences in the kinetics and amplitude of Ca^{2+} transients between both species, implying species-specific sensitivity for different stress conditions. The potato line generated in this work provides a useful tool for further investigations on stress-induced signalling pathways, which could contribute to the generation of novel, stress-tolerant potato varieties.

Keywords Potato, *Arabidopsis thaliana*, Crops, Calcium signalling, Aequorin, Stress perception

Plants sense and respond to unfavourable environmental conditions to mitigate the negative effects of such stresses. Indeed, each stress type and each stress combination cause a unique molecular footprint, which induces a fine-tuned cellular response[1,2]. For example, unique stress-specific transcriptional changes have been observed in response to heat, drought, high light, or combinations of these treatments in the model plant *A. thaliana*[3,4]. Secondary messengers are involved in transducing a primary stimulus into an appropriate cellular response. In plants, changes in the concentration of free Ca^{2+} in the cytosol (referred here as $[Ca^{2+}]_{cyt}$), but also in various organelles, have emerged as a universal secondary messenger[5–7]. A wide range of stresses as well as developmental processes trigger temporal increases in $[Ca^{2+}]_{cyt}$ by an influx of Ca^{2+} from external and internal stores. The amplitude and timing of Ca^{2+} influx depends on the type of perturbation, the magnitude of the stress and how often the plant faced such stress conditions in the past[8,9], resulting in an information encoding 'calcium signature'[10,11]. So far, calcium signatures have been described in Arabidopsis, for instance in response to oxidative stress, biotic elicitors, osmotic stress, salt, cold or touch[9,12–16].

The use of the genetically encoded Ca^{2+} indicator (GECI) apoaequorin to determine absolute concentrations of free Ca^{2+} in plants was established in the 1990s in Arabidopsis[12] and has since been used to investigate Ca^{2+} changes in many studies[17]. However, only few studies have reported the use of GECIs in crop species, such as H_2O_2 and NaCl responses in rice roots[18], chilling response in winter wheat[19], infection with *Cuscuta reflexa* in tomato[20], and a set of stressors in barley[21]. The comparison of Ca^{2+} transients between those species revealed tissue- and species-specific calcium signatures in response to different stress stimuli, which might be related to species-specific sensitivity to each stressor or to differences in the down-stream responses.

Plants show different sensitivity to environmental factors depending on their genetic make-up, which defines stress adaptation and acclimation. Potatoes are cultivated in nearly all regions of the world and are an important factor for global nutrition[22]. However, potato plants originate from an area with particular conditions, the high altitudes of the Andes. Based on its origin, potato growth, and by that also tuber yield, is quite sensitive to a wide range of environmental factors, including elevated temperatures[23] and salinity[24]. So far, Ca^{2+} signals have only

[1]Institute for Cellular and Molecular Botany, University of Bonn, Kirschallee 1, 53115 Bonn, Germany. [2]Department of Biosciences, Durham University, South Road, Durham DH1 3LE, UK. [3]Department of Biology, Chair of Biochemistry, Friedrich-Alexander-University Erlangen-Nuremberg, Staudtstraße 5, Erlangen 91058, Germany. ✉email: adieren@uni-bonn.de; vothknecht@uni-bonn.de

been investigated in response to flagellin 28 (flg-28) in potato plants[25]. To obtain a more comprehensive overview, we generated transgenic potato lines expressing apoaequorin under the control of the cauliflower mosaic virus (CaMV) 35S promoter and determined calcium signatures in response to different abiotic and biotic stimuli in leaf tissue of soil-grown plants. We performed direct comparisons with Ca^{2+} responses in Arabidopsis in order to put the results obtained for potato in context of the vast knowledge available from this model plant.

Results

Generation and characterisation of transgenic potato lines expressing *apoaequorin*

To measure stimuli-induced $[Ca^{2+}]_{cyt}$ changes in vivo in potato plants, three independent transgenic potato lines (*Solanum tuberosum* L. cv. Désirée) carrying the p35S::apoaequorin construct were created (Fig. 1; Supplementary Fig. S1), referred to hereafter as St-AEQ_{cyt}. Protein extracts from all lines showed aequorin luminescence in response to discharge solution (25 mM $CaCl_2$) after overnight reconstitution with coelenterazine (Fig. 1a) indicating expression of the apoaequorin protein. Different luminescence levels were observed among the three St-AEQ_{cyt} lines, with #20 showing the highest luminescence level, and this line was therefore used for all further experiments. Functionality of the sensor *in planta* could be confirmed by measuring Ca^{2+} induced Ca^{2+} transients (Fig. 1b). Importantly, the insertion of the construct into the genome and expression of apoaequorin did not have any visible impact on growth and development in comparison to wild type plants (Fig. 1c and d). Western Blot analysis confirmed the presence of the apoaequorin protein in leaf extract (Supplementary Fig. S1a). The comparison to a previously described Arabidopsis line carrying the same *35S::apoaequorin* construct (At-AEQ_{cyt}) showed a lower expression level of apoaequorin (Supplementary Fig. S1a). Accordingly, only about 25% of the aequorin luminescence in response to discharge solution was observed in St-AEQ_{cyt} lines compared to At-AEQ_{cyt} (Supplementary Fig. S1b).

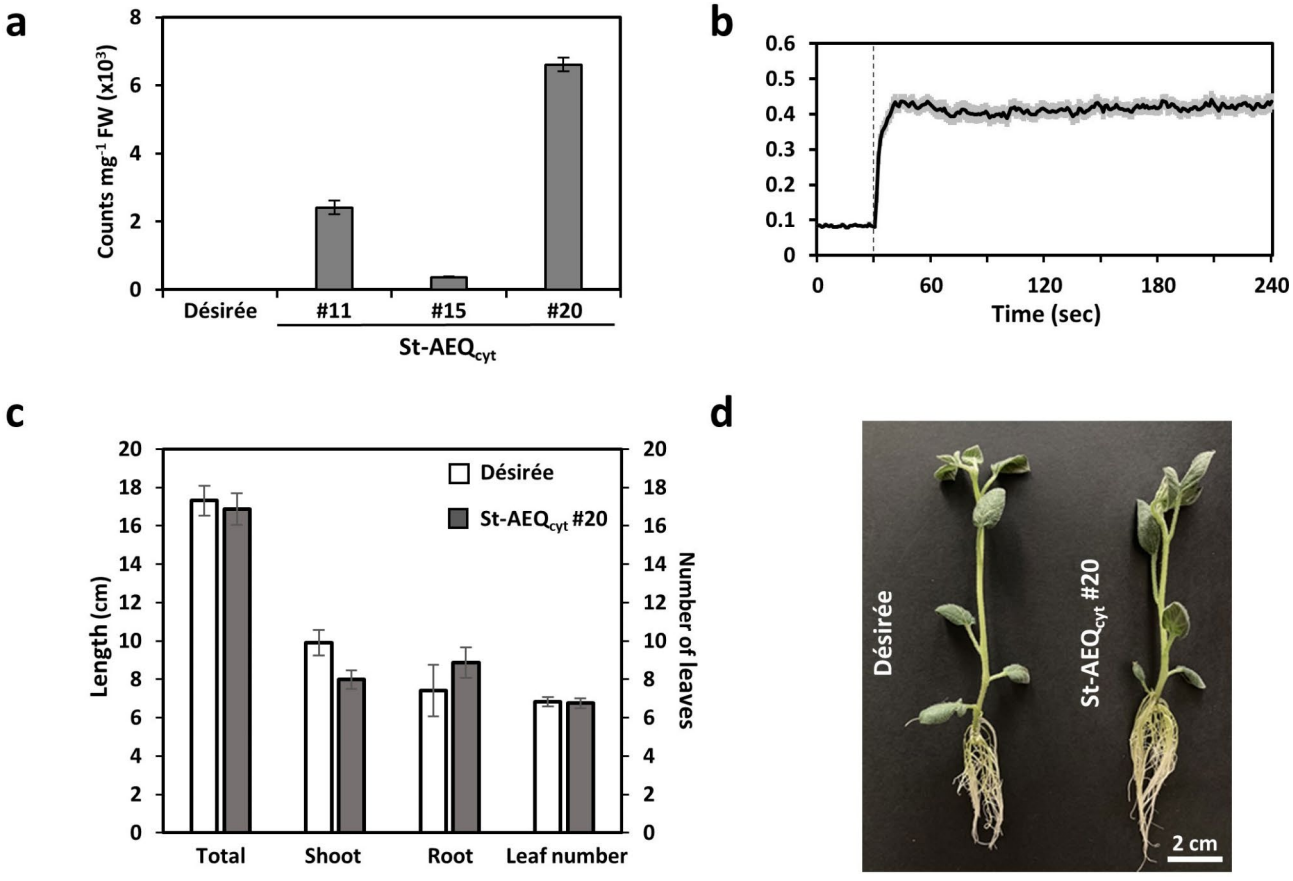

Fig. 1. Selection and characterisation of St-AEQ_{cyt} lines. (**a**) Photon counts (average counts 10 s after adding 50 mM $CaCl_2$) were measured in leaf extracts from three independent transgenic potato St-AEQ_{cyt} lines after in vitro reconstitution of aequorin with coelenterazine. Untransformed potato cultivar Désirée was used as a negative control ($n = 9$, mean ± SE). (**b**) Time course of changes in $[Ca^{2+}]_{cyt}$ in leaf discs from St-AEQcyt #20 in response to external Ca^{2+} application (final concentration 500 mM). (**c**) Comparison of the total plant length, root length, shoot length, and number of leaves in three-week old St-AEQ_{cyt} #20 and wildtype Désirée plants ($n = 8$, mean ± SE). (**d**) Representative picture of three-week old Désirée wild type and St-AEQ_{cyt} #20 plant.

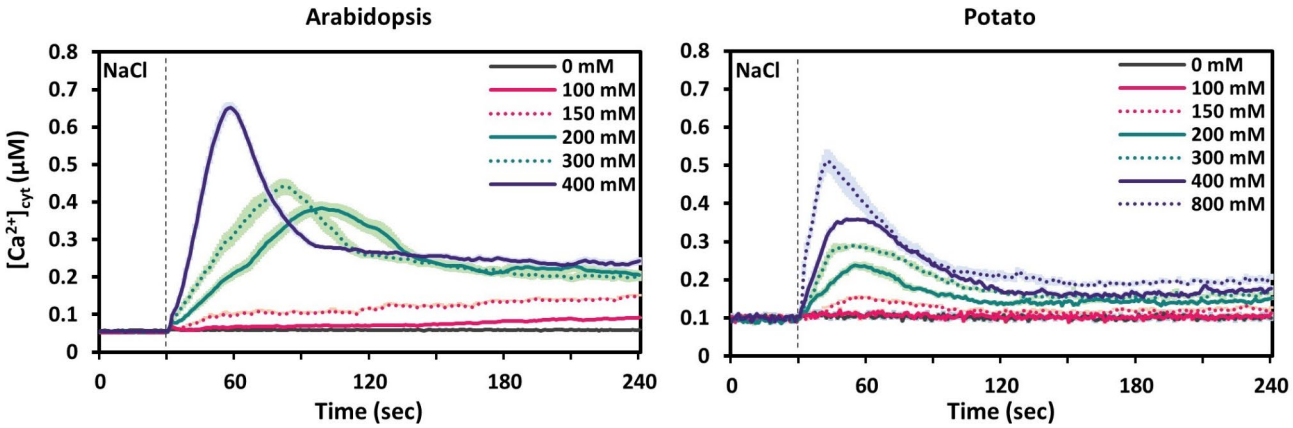

Fig. 2. Time course of changes in $[Ca^{2+}]_{cyt}$ in response to different concentrations of NaCl in leaf tissue of Arabidopsis (left) and potato (right) plants. Values are shown as mean ± SE ($n = 9$). Dashed vertical lines indicate the time point of stimuli application (30 s).

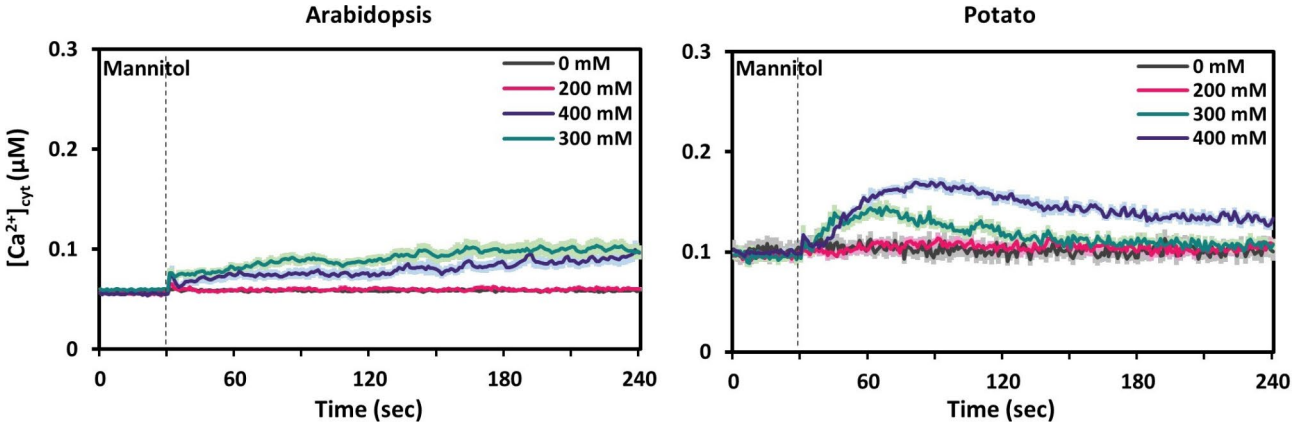

Fig. 3. Time course of changes in $[Ca^{2+}]_{cyt}$ in response to different concentrations of mannitol in leaf tissue of Arabidopsis (left) and potato (right) plants. Values are shown as mean ± SE ($n = 9$). Dashed vertical lines indicate the time point of stimuli application (30 s).

Calcium signatures in Arabidopsis and potato in response to abiotic stimuli

We first analysed stress-induced calcium signatures in leaf discs of Arabidopsis (At-AEQ_{cyt}) and potato (St-AEQ_{cyt}) in response to the abiotic factors salinity, drought and oxidative stress (Figs. 2, 3 and 4). To that end we treated leaf discs from plants of similar age grown on soil with NaCl, mannitol and H_2O_2.

Salt stress (NaCl)

Initially the salt response was tested in steps of a two-fold increase starting with 100 mM NaCl (Fig. 2). In both species, NaCl elicited a strong response after application of concentrations above 200 mM NaCl, but the kinetics of the response differed between the two species. In Arabidopsis, 200 mM NaCl produced a broad peak occurring at around 70 s after application with a maximum $[Ca^{2+}]_{cyt}$ amplitude of 0.38 µM (Fig. 2, Arabidopsis, green solid line). Increasing the NaCl concentration to 400 mM further enhanced the amplitude to 0.65 µM $[Ca^{2+}]_{cyt}$ and shifted the time of the maximum peak to around 30 s after application (Fig. 2, Arabidopsis, purple solid line). The shift in the timepoint of the peak value in response to increasing NaCl concentrations made us decide to test the response also to intermediate NaCl concentrations (Fig. 2, Arabidopsis, dotted lines), resulting in true interjacent responses. By testing all these different concentrations, we were able to visualise the dose-dependent shaping of the curve towards a stronger and faster response. Neither time nor amplitude of the maximum peak value did alter any more at concentrations above 400 mM.

In potato, application of NaCl also triggered clear Ca^{2+} transients (Fig. 2, potato), albeit with a slightly lower amplitude than in Arabidopsis. Also potato showed a dose-dependent increase in the amplitude of the $[Ca^{2+}]_{cyt}$ peak, however, the timing of the $[Ca^{2+}]_{cyt}$ peak only showed a very minor shift (Fig. 2, potato). In contrast to Arabidopsis, 800 mM NaCl (Fig. 2, potato, purple dotted line) was needed to induce a maximum response of 0.5 µM $[Ca^{2+}]_{cyt}$, comparable in height and shape to the response to 400 mM NaCl in Arabidopsis. Overall, these

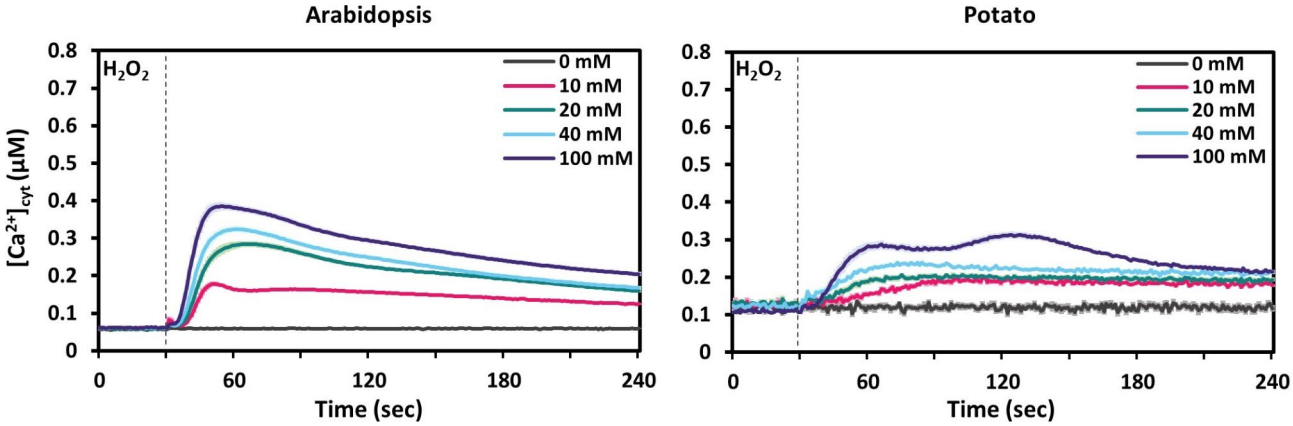

Fig. 4. Time course of changes in $[Ca^{2+}]_{cyt}$ in response to different concentrations of H_2O_2 in leaf tissue of Arabidopsis (left) and potato (right) plants. Values are shown as mean ± SE ($n = 9$). Dashed vertical lines indicate the time point of stimuli application (30 s).

data show that dose-dependent NaCl-induced Ca^{2+} transients occur in both species, but they show differences in their kinetics.

Osmotic stress (Mannitol)

To investigate the calcium signature of Arabidopsis and potato in response to acute osmotic changes, we recorded free $[Ca^{2+}]_{cyt}$ in leaf discs upon application of different concentrations of mannitol (Fig. 3). Because of the crystallizing properties of mannitol at higher concentrations, and the fact that we have to inject a two-fold concentrated stock solution via a narrow syringe system, the concentrations that we could test were limited to a maximum of 400 mM.

In Arabidopsis, a mannitol application with a concentration of 200 mM did not result in any response. Also higher concentrations (300 and 400 mM) did not induced a clear Ca^{2+} spike but led to a long-lasting minor elevation of $[Ca^{2+}]_{cyt}$ throughout the whole measurement period (240 s). This elevation started immediately after application of the stimulus and steadily increased to about 0.05 µM $[Ca^{2+}]_{cyt}$ (Fig. 3, Arabidopsis). In contrast to Arabidopsis, we observed a small but clear Ca^{2+} spike in potato at a concentration of 300 mM with a maximum amplitude of 0.15 µM $[Ca^{2+}]_{cyt}$ at about 30 s after application (Fig. 3, potato). At 400 mM the amplitude of the response increased further, and the peak value was reached later (60 s after application).

Oxidative stress (H_2O_2)

Oxidative stress is a common result of unfavourable growth conditions but also certain biotic stimuli induce an oxidative burst[26]. Hydrogen peroxide (H_2O_2) is considered as the predominant signalling molecule during oxidative stress, due to its stable nature (half-life > 1 ms) compared to other reactive oxygen species[27]. Therefore, we used H_2O_2 as a stimulus to analyse $[Ca^{2+}]_{cyt}$ changes in response to oxidative stress (Fig. 4).

In Arabidopsis, H_2O_2 treatment with the lowest tested concentration (10 mM) resulted directly in a clear peak-shaped response with a maximum amplitude of 0.2 µM $[Ca^{2+}]_{cyt}$ just 15 s after application. The peak value of $[Ca^{2+}]_{cyt}$ increased in a dose-dependent manner with a maximal response of 0.4 µM observed at 100 mM (Fig. 4, Arabidopsis, purple line). In potato, 10 mM H_2O_2 did not elicit a clear Ca^{2+} transient but a slow minor increase (Fig. 4, potato, pink line) similar to what was observed in Arabidopsis in case of mannitol. At 20 mM H_2O_2 a peak-like shape started to appear, which turned into a double-peaked calcium signature at 100 mM H_2O_2 (Fig. 4, potato, purple line). The first peak occurred at around 30 s after application, similar to the peak seen in Arabidopsis, however, its amplitude was much lower (0.3 µM). The second peak was slightly higher than the first, occurred at around 90 s after application, was not visible in Arabidopsis plants (Fig. 4, Arabidopsis), and was also not seen in barley[21].

Calcium signatures in response to PAMPs

Various studies have demonstrated that Ca^{2+} signals together with an apoplastic ROS-burst play an important role in activating the plant's pathogen defence system[28,29]. Changes in $[Ca^{2+}]_{cyt}$ are thus an early and essential element in intracellular signalling networks after perception of pathogen-associated molecular patterns (PAMPs). Due to the observed species-specific Ca^{2+} transients in response to H_2O_2, we decided to also analyse $[Ca^{2+}]_{cyt}$ changes in response to two biotic elicitors (Fig. 5a-b). Compared to the abiotic stimuli, responses to the biotic components were generally slower (Fig. 5c) and measurements were taken for longer periods.

Flg22

Flg22 is a 22 amino acid long fragment of the *Pseudomonas syringae* flagellin whose induction of Ca^{2+} transients and triggering of ROS production has been described in different plant species and tissues[30–32]. While an increase in $[Ca^{2+}]_{cyt}$ occurred already at 0.5 µM flg22 in Arabidopsis, a clear peak was observed with concentrations of 1 µM and higher (Fig. 5a, Arabidopsis). A maximal amplitude of less than 0.2 µM $[Ca^{2+}]_{cyt}$ was observed at around

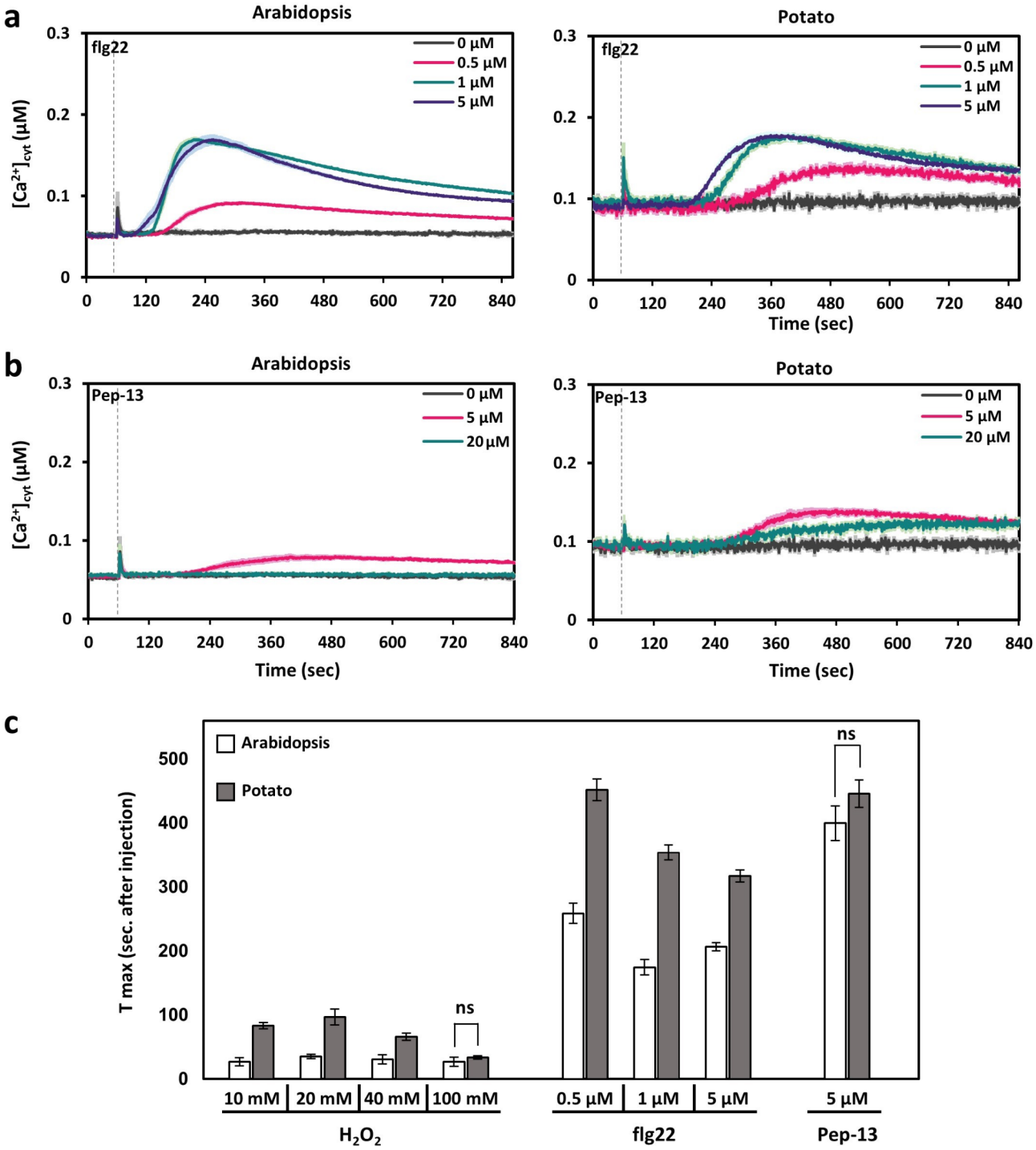

Fig. 5. Induction of Ca^{2+} signals in response to pathogen-associated molecular patterns (PAMPs) in leaf tissue of Arabidopsis and potato. (**a**) Time course of $[Ca^{2+}]_{cyt}$ in Arabidopsis (left) and potato (right) in response do different concentrations of flg22. (**b**) Time course of $[Ca^{2+}]_{cyt}$ in Arabidopsis (left) and potato (right) in response do different concentrations of Pep-13. Values are shown as mean ± SE ($n = 9$). Dashed lines indicate the time point of PAMP application (60 s). (**c**) Time to reach the maximal increase of $[Ca^{2+}]_{cyt}$ (T_{max}) after application of flg22 and Pep-13 in comparison to H_2O_2. Values are derived from the data in Figs. 4 and 5A, and 5B. Treatments that resulted in non-significant differences between the two species are indicated (two tailed student's t-test, $p \leq 0.01$).

160 s after application, similar to what has been described earlier in Arabidopsis[21,33] and the peak declined slowly (Fig. 5a, Arabidopsis). The $[Ca^{2+}]_{cyt}$ transient in potato in response to flg22 looked similar but the response was even slower than in Arabidopsis. Its elevation started only 3 min after application with a peak time around 300s (Fig. 5a, potato and Fig. 5c), which is similar to what was described for barley[21]. In both species, the time it took to reach the maximum amplitude after application of the flg22 stimulus (T_{max}) was much longer than the response to the direct H_2O_2 application (Fig. 4), independent of the concentration tested (Fig. 5c). This could be due to flg22 inducing ROS production which subsequently, and thus time-delayed, triggers a Ca^{2+} transient.

Pep-13

We also tested $[Ca^{2+}]_{cyt}$ changes in response to Pep-13, a fragment of a glycoprotein from the late blight-causing *Phytophthora infestans*. Arabidopsis showed only a very minor increase in $[Ca^{2+}]_{cyt}$ of less than 0.04 µM with 5 µM elicitor and no response at higher concentrations (Fig. 5b, Arabidopsis). The response in potato to 5 µM Pep-13 was similar but with a higher amplitude of 0.05 µM. At 20 µM Pep-13, the response was lower and similar to what was observed in Arabidopsis at 5 µM (Fig. 5b, potato). The time to the maximum increase in $[Ca^{2+}]_{cyt}$ was even longer than with flg-22 and was observed 6 min after application (Fig. 5c). What we did not observe was a slower response of potato compared to Arabidopsis as seen for flg22. (Fig. 5c)

In vivo imaging of $H2O_2$induced redox changes using potato biosensor plants

When analysing the Ca^{2+} response of Arabidopsis and potato to H_2O_2, we observed a marked difference in timing and amplitude between the two species (Fig. 4). We were wondering whether this is caused by *bona fide* differences in the molecular response to equivalent redox changes, or whether our treatments induced different redox changes in the two species. To address this question, we expressed the redox-sensitive Grx1-roGFP2 sensor under control of the 35S CaMV promoter in the same cultivar (Désirée) as used for the Ca^{2+} analyses (Fig. 6; Supplementary Fig. S2-S4). Several independent lines were obtained that showed a strong and reliable emission at 510 nm upon excitation at 485 nm under reducing conditions (Supplementary Fig. S2). Grx1-roGFP2 line #29 was used for subsequent analysis. It revealed a clear fluorescence signal throughout the leaf with stronger signals in the main leaf veins when imaged under blue light (460–490 nm) using a fluorescence imager (Fig. 6a). Expression of Grx1-roGFP2 had no visible effect on the growth of this line compared to wild type and Western Blot analysis confirmed the presence of the Grx1-roGFP2 protein (Fig. 6b; Supplementary Fig. S3).

Confocal laser scanning microscopy of leaf discs of Grx1-roGFP2 confirmed the cytosolic localisation of the sensor (Fig. 6c). Reducing conditions induced by 100 mM DTT only resulted in minor changes of the fluorescence signals observed at 535 ± 15 nm after excitation at either 405–485 nm. Oxidation by 100 mM H_2O_2 lowered the emission upon excitation at 485 nm and clearly increased the emission upon excitation at 405 nm (Fig. 6c). Together this shows that the sensor line can be used to assess the cytosolic oxidation status.

Further analyses were performed using the same plate luminometer employed for the aequorin measurements. Comparison of soil grown Grx1-roGFP2 plants from potato with Grx1-roGFP2-expressing Arabidopsis[34] without any stress treatment showed a nearly three times higher ratio of 405/485 nm fluorescence in potato (Fig. 6d, mock). The biosensor is most sensitive for the oxidation status of the small antioxidant glutathione (GSH); thus, the data indicate a higher basal GSH oxidation in potato. Treatment of Arabidopsis and potato with DTT revealed only minor changes in the 405/485 nm ratio with 10 mM DTT and no further decrease with 100 mM DTT or higher (Fig. 6d; Supplementary Fig. S4). This confirms the data from the microscopic analysis of potato (Fig. 6c) and demonstrates that 100 mM DTT fully reduces the leaf cytosolic GSH for both species.

Arabidopsis and potato show slightly differences under treatment with H_2O_2. Both species reached a maximum 400/485 nm ratio and thus full oxidation of the cytosol at 100 mM H_2O_2. However, upon treatment with 10 mM H_2O_2, Arabidopsis leaf cells showed a significant increase in ratio of 405/485 nm fluorescence, while in potato no significant difference to the mock value was observed (Fig. 6d). After treatment with 100 mM H_2O_2, the ratio of 400/485 nm fluorescence showed a further increase in Arabidopsis and a significant increase in potato. No further increase in ratio was observed with higher H_2O_2 concentrations for either species. Thus, the full dynamic range could be achieved for both species with 10 mM DTT and 100 mM H_2O_2, however, while in Arabidopsis the ratio of 405/485 nm fluorescence increased from 0.2 to 0.6 (dynamic range of ~ 3), potato only showed less than a duplicating of the ratio from 0.55 to 0.9 (Fig. 6d). This indicates quite a strong difference in GSH oxidation between Arabidopsis and potato and the high level of GSH oxidation might play a part in the lower H_2O_2-induced Ca^{2+} response that we observed in potato (Fig. 4b).

Discussion

Transient changes in the concentration of $[Ca^{2+}]_{cyt}$ are among the earliest responses of plant cells to many environmental stresses. Intriguingly, the exact dynamics of the Ca^{2+} signature not only differs depending on the stimulus but can also differ between stress acclimated and non-acclimated plants[9]. This raises the exciting possibility that screening of specific Ca^{2+} signatures could identify promising varieties for improved crop breeding. However, before such an approach could be incorporated into breeding programmes, baseline Ca^{2+} responses for the desired crop need to be investigated. Considering the importance of Ca^{2+} signalling as a very early component of plant stress responses, surprisingly few investigations using GECIs have so far been performed with plants other than Arabidopsis[18–21,35]. As part of an large-scale analysis of molecular and phenotypical responses of potatoes to environmental stress (https://adapt.univie.ac.at/), we thus investigated stress-dependent changes in $[Ca^{2+}]_{cyt}$ in the moderate stress-resistant potato variety Désirée. To better put our data in the context of what is known in the model plant Arabidopsis, we measured all stress responses in parallel between both plants. This avoids as much as possible issues, such as difference in plant age, growth conditions etc. when comparing to already published data. Although the apoaequorin expression level was lower and aequorin-derived photon counts in potato reached only about 25% as those observed in Arabidopsis (supplementary Fig.

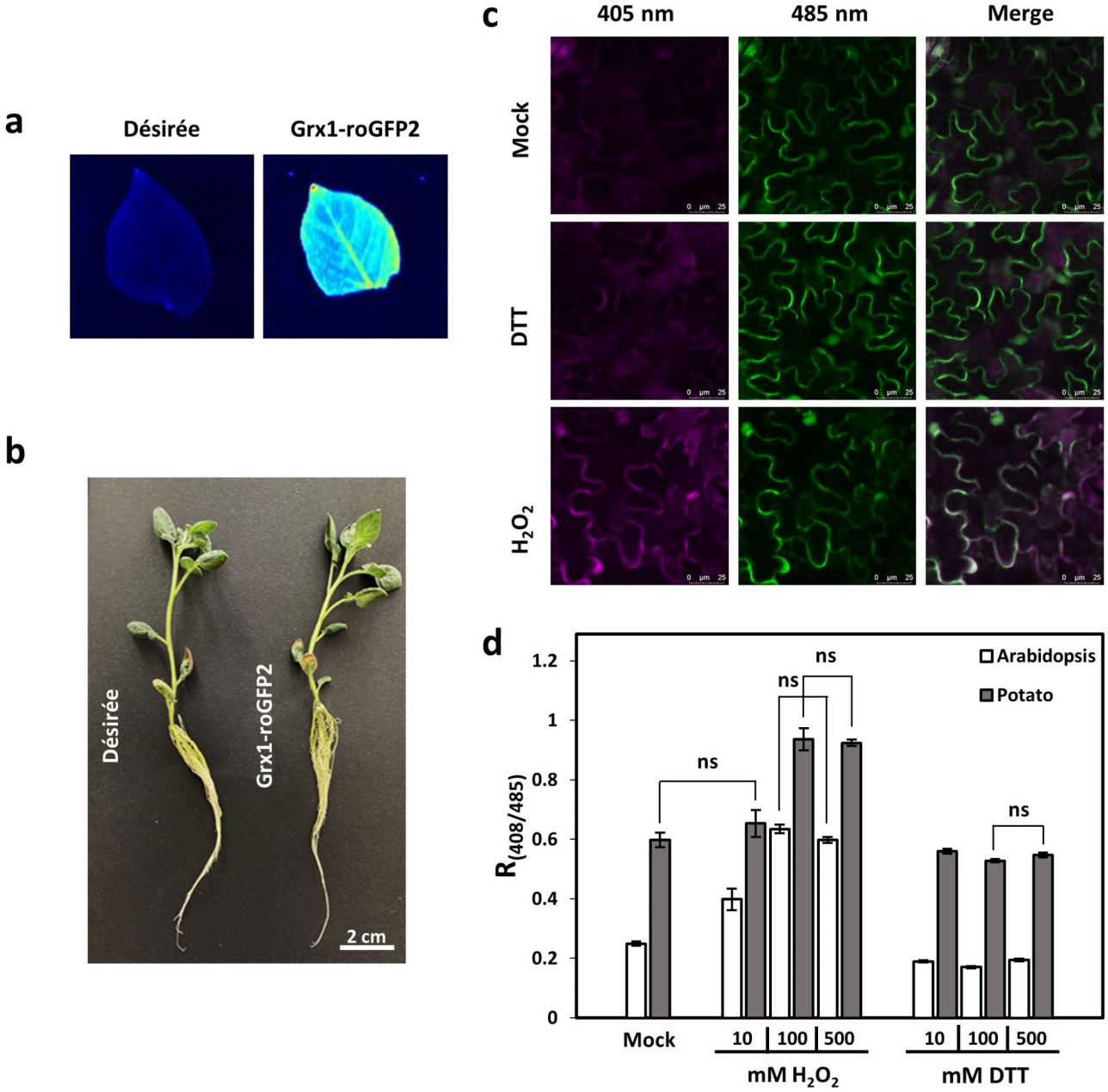

Fig. 6. Cytosolic redox status of soil-grown potato and Arabidopsis plants. (**a**) Image of the abaxial side of full mature leaves of wild type and St-Grx1-roGFP2 plants after excitation with blue light (460–485 nm). (**b**) Representative picture of three-week old Désirée (wild type) and St-Grx1-roGFP2 potato plants. (**c**) Confocal images of St-Grx1-roGFP2 plants after sequential excitation at 405 nm, 485 nm, and the merge of both channels. Leaf discs were incubated for 10 min in either mock solution, 100 mM DTT or 100 mM H_2O_2. (**d**) Ratiometric measurement of emission at 535 ± 15 nm after sequential excitation at 405 nm and 485 nm. Leaf discs were placed with abaxial side upwards into 96-well plates and emission was measured 10 min after application of imaging buffer (mock), H_2O_2 (10, 100 or 500 mM) or DTT (10, 100 or 500 mM) ($n = 9$, mean ± SE). Treatments that resulted in non-significant differences within the same species are indicated (two tailed student's t-test, $p \leq 0.01$).

S1a and b), we could measure well-defined responses in the potato line #20 with stress-induced photon counts well above baseline levels. Thus, we believe that the differences we observed represent species-specific responses of potato and Arabidopsis.

With regards to NaCl, the differences between Arabidopsis and potato mostly pertained to the shape of the response curve at different concentrations (Fig. 2). While both organisms showed a clear dose dependent response to NaCl, Arabidopsis exhibited a strong shift in the maximum peak which was reached earlier with higher concentrations. By contrast, this effect of concentration was very minor in potato. Ultimately, both species reached a similar shape of the response curve, however, potato required about double the NaCl concentration for

a maximal response and even then, a much lower peak value for $[Ca^{2+}]_{cyt}$ was recorded. The much lower NaCl response in potato is remarkable since potato plants have been described as rather sensitive to salt stress with a soil salinity threshold of 1.7 dSm^{-1}. This is remarkably low in comparison to more NaCl-insensitive crops such as wheat (6 dSm^{-1}) and barley (8 dSm^{-1})[24], the latter of which shows a NaCl-induced Ca^{2+} transient in its leaves with a maximum amplitude of around 0.4 µM[21]. The salt overly sensitive (SOS) pathway plays a crucial role in the salt tolerance of plants and involves the activation of a N^+/H^+ antiporter by a Ca^{2+}-dependent sensor-protein kinase complex[36]. Very little is known about the SOS pathway in potato[37]. Whether the lower Ca^{2+} transient in potato leads to less activation of the SOS pathway and therefore impacts subsequent salt tolerance remains to be tested, especially because Arabidopsis displays a high NaCl-induced Ca^{2+} transient but is also considered as salt sensitive. While such species-specific sensitivity to salt might have an impact on the Ca^{2+} responses they are not sufficient to fully explain these observations, especially in light of the fact that salt stress occurs primarily as soil salinity and is sensed in the roots[38]. Consequently, very little is known about salt sensing in leaves and shoots. Another reason for the observed differences in Ca^{2+} responses could lie in different physical surface properties of the leaves that affect the uptake of NaCl, however NaCl penetration into the tissue cannot be easily accessed experimentally.

In contrast to NaCl, mannitol is a non-ionic, osmotic substance. It is used to mimic drought stress since the latter is often not applicable in experimental set-ups, such as the one used in this study. Increase in $[Ca^{2+}]_{cyt}$ in response to mannitol has been shown in several previous studies for whole young seedlings of Arabidopsis[13,39,40]. However, when roots and shoots were analysed separately, it was shown that the response occurred exclusively in roots while no $[Ca^{2+}]_{cyt}$ transient could be observed in leaves neither in Arabidopsis nor in barley[21,41]. In this study the lack of response in leaves could be confirmed for Arabidopsis also in case of soil-grown plants (Fig. 3). By contrast, a broad $[Ca^{2+}]_{cyt}$ transient could be observed in response to 400 mM in the leaf tissue of potato. The underlaying mechanisms for these species-dependent responses to mannitol need to be further investigated at a molecular level.

With regards to H_2O_2, it was most remarkable that for both species rather high concentrations were required to elicit a response. In experiments using leaves from young seedlings grown on sterile medium, 10–15 mM H_2O_2 was sufficient for a maximal response in Arabidopsis and barley[21], while in the leaves of soil-grown, older plants used in this study the amplitude of $[Ca^{2+}]_{cyt}$ increased up to 100 mM H_2O_2 for both Arabidopsis and potato. This might be due to a difference in penetration of H_2O_2 into the tissue of the older, soil-grown plants. Moreover, while Arabidopsis showed response curves with a dose-dependent increase in the maximal amplitude but identical shape, the response curve in potato became biphasic with two overlapping broad peaks of similar amplitude. The timing of the first of these two peaks matched the single peak seen in Arabidopsis indicating that they are caused by the same initial response to H_2O_2. The second peak in potato could be attributed to secondary responses that are activated by the initial increase in $[Ca^{2+}]_{cyt}$. Biphasic signature have been described before also for Arabidopsis in response to ozone or even H_2O_2[14,42] however, in these studies, whole seedlings including roots were used and the second peak occurs much later (~600s after application) than what we observe with potato. Thus, the molecular basis for the biphasic response of potato is likely different. In this regard, the differences we measured for the basal oxidative state of the cytosol using the GRX1-roGFP2 sensor lines for Arabidopsis and potato (Fig. 6d) is interesting. Our data shows that both species have the potential to reach a similar increase of the oxidative state (+0.4 $R_{405/485}$) after being stimulated with 100 mM H_2O_2. However, the reason behind the higher basal level of $R_{405/485}$ (0.2 vs. 0.55) in potato remains unclear. Former research with a chloroplast-targeted GRX1-roGFP2 probe in potato[43] revealed that the basal oxidative state of the chloroplast was higher for older leaves compared to younger leaves and they speculated that this may be due to an increase in photosynthesis efficiency and decrease in photoprotection.

Differences between Arabidopsis and potato where also observed for the two PAMPs, flg22 and Pep-13. Most remarkable was the response to Pep-13, which contrary to most other stimuli we tested in the present study, elicited a higher $[Ca^{2+}]_{cyt}$ increase in potato than in Arabidopsis, suggesting that potato has a higher sensitivity to Pep-13 and thus *Phytophthora infestans*. Indeed, late blight, caused by *Phytophthora infestans*, is the most devastating disease of global potato production[44]. It was however shown before that Pep-13 elicits a defence response against late blight in parsley including a $[Ca^{2+}]_{cyt}$ transient with a peak of about 0.8 µM at around 150 s[45,46]. This response is faster and stronger than what we observed in Arabidopsis and potato (Fig. 5b). This might be the result of the different types of sample tissue used (parsley suspension cells vs. leaf tissue from soil grown plants) or could indicate a high susceptibility of parsley to *Phytophthora*. Indeed, severe yield loss of parsley due to root rot caused by *Phytophthora cryptogea* has been described[47].

Overall, when comparing the interplay between species- and stimulus-dependent responses, no simple conclusion as to the driving factor of the observed differences can be drawn. While issues such as difference in stimuli-penetration need to be addressed methodically, it can be expected that species-specific differences in Ca^{2+} transients affect the downstream mechanism of perception and translation of the stimulus into cellular responses. Mechanistically, Ca^{2+} signatures are shaped by the activity of Ca^{2+} transporters and channels, as well as Ca^{2+}-buffering systems[48].

The phylogenetic relationship between Ca^{2+} transport proteins across a range of plant species has been determined[49] and based on this analysis, we identified similar sequences in the potato reference genome Phureja DM1-3 v6.1 (Supplementary Table S1). Notably, the potato genome seems to encode more GLRs (27 in potato vs. 20 in Arabidopsis), MCA channels (7 vs. 2) and Ca^{2+}-ATPases (21 vs. 14). However, given the overall higher number of annotated protein-coding genes in potato compared to the Arabidopsis genome[50] these differences are not significant (chi-square test, $p < 0.05$). Nevertheless, variance in the Ca^{2+} toolbox between species might be related to some of the observed difference in stress-induced Ca^{2+} transients and the functionality of the corresponding gene products and the impact of a putatively increased complexity in potato remain to be studied further. With regard to down-stream mechanisms activated by the Ca^{2+} transients, an alteration in amplitude

and/or shape could affect how different plants can cope with environmental changes. This could be investigated by analysing the Ca^{2+} response of different varieties of the same species that are more or less susceptible to a certain stress. In that regard, our data can be used to define which stimuli and stimuli concentrations are useful to trigger cytosolic Ca^{2+} changes in the moderate stress-resistant potato variety Désirée and by that offers a basis for future Ca^{2+} related studies in this crop species.

Methods

Vector construction and transformation into*S. tuberosum*(cv. Désirée)

To generate potato lines of the cultivar Désirée with constitutive expression of *apoaequorin* (St-AEQ_{cyt}), the pMAQ2 vector carrying the coding region of *apoaequorin* down-stream of the cauliflower mosaic virus (CaMV) 35S promoter was used[12]. For the generation of Désirée lines with constitutive expression of redox-sensitive *roGFP2* fused with human *glutaredoxin 1* (St-Grx1-roGPF2) a previous described fusion construct[51] was inserted into pBINar upstream of the CaMV 35S promoter. Both constructs were introduced into the potato cultivar Désirée as described previously[52].

Plant material and growth conditions

In addition to the transgenic potato plants described above, corresponding transgenic *A. thaliana* plants (Col-0) expressing either cytosolic *apoaequorin* (At-AEQ_{cyt};[12]) or *Grx1-roGFP2* (St-Grx1-roGFP2[53]) under the control of the cauliflower mosaic virus 35S promoter were used.

Potato cuttings/explants were first grown on sterile MS agar (pH 5.7, 2% (w/v) sucrose) for root formation and subsequently transplanted into single pots filled with soil. In case of Arabidopsis, seeds were sown onto the same soil, stratified for 2 days at 4 °C in the dark, and separated after germination into single pots. Potato and Arabidopsis plants were subsequently cultivated side-by-side for 3 weeks in a growth chamber with a temperature of 20 ± 2 °C at a light intensity of ~ 150 µmol photons m^{-2} s^{-1} (Philips TLD 18 W of alternating 830/840 light colour) under long day (16 h light/8 h dark) conditions.

In vitro aequorin reconstitution and quantification

To quantify *apoaequorin* expression in transgenic potato plants, aequorin was reconstituted and chemiluminescence was measured in vitro. Leaf discs (Ø 6 mm) were collected from fully expanded leaves of soil-grown St-AEQ_{cyt} plants and the fresh weight was recorded. The tissue was homogenised in 500 µL extraction buffer (0.5 M NaCl, 9.547 mM beta-mercaptoethanol, 5 mM EDTA, 0.2% (w/v) gelatine, 10 mM Tris-HCl pH 7.4) and cleared by centrifugation in a bench-top centrifuge at 16,300 *g* for 10 min. Supernatants were transferred to new tubes and reconstituted with 1 µM coelenterazine (Biosynth AG, Switzerland) at room temperature in the dark overnight. The following day, 4 µL aliquots were added to 200 µL of 200 mM Tris HCl, 0.5 mM EDTA, pH 7.0 in the wells of a 96 well plate. The relative amount of aequorin in each extract was calculated by measuring photon counts over a 10-second period before and after addition of 200µL of 50 mM $CaCl_2$ (final concentration 25 mM), using a plate luminometer (Tristar 3 Multimode Reader, Berthold GmbH). Aequorin abundance was expressed as relative luminescence / fresh weight (arbitrary units/mg).

Aequorin and GFP immunodetection

Proteins were isolated from leaves of 3-week-old potato plants using Lacus protein isolation buffer (20 mM Tris pH 7.7, 80 mM NaCl, 0.75 mM EDTA, 1 mM $CaCl_2$, 5 mM $MgCl_2$, 1 mM DTT, 2% (w/v) SDS). The proteins were separated on a 12% SDS-polyacrylamide gel and transferred to nitrocellulose membrane (0.45 µm pore size). After transfer of the proteins the membrane was stained using 0.1% (w/v) Ponceau S in 5% (v/v) glacial acetic acid. Immunodetection was performed using antibodies against aequorin (Abcam, Berlin, Germany) or GFP (Agrisera, AS20 4443) and an ECL detection system with an anti-rabbit secondary antibody coupled to horseradish peroxidase.

In planta reconstitution of apoaequorin and stimuli-induced luminescence measurements

One day before measurements were taken, leaf discs (Ø 6 mm) were collected from ~ 3-week-old plants and floated overnight in the dark at 20 °C in 10 µM coelenterazine (Biosynth AG, Switzerland) for reconstitution. The following day, the leaf discs were transferred individually into a 96-well plate containing 100 µL ddH_2O. Photon count measurements were performed using a plate luminometer (Tristar 2 Multimode Reader, Berthold GmbH). The basal level of photon counts was measured for 30 s for the abiotic stimuli and 60 s for the PAMPs (Flg22, GenScript Biotech Corporation, The Netherlands; Pep-13, ProteoGenix, France) with an interval of 1 s, followed by application of various stimulants using a stock solution with 2x the final concentration and a volume equal to the starting volume (100 µL), with continuous measuring for a minimum of 240 s after application. Subsequently, the remaining aequorin was discharged by adding 1/3 volume of 3 M $CaCl_2$ in 30% (v/v) EtOH resulting in a final concentration of 1 M $CaCl_2$ in 10% (v/v) EtOH. Photon counts were then recorded for another 300 s. $[Ca^{2+}]_{cyt}$ was calculated based on the photon counts as described previously[54].

Measurement of Grx1-roGFP2 fluorescence

To check the expression of Grx1-roGFP2 in leaves of 3-week-old wild type and St-Grx1-roGFP2, plants were imaged via the ChemiDoc MP Imaging System (BioRAD, USA) with a blue light source (460–490 nm) and an exposure time of 0.4 s.

For imaging of Grx1-roGFP2 fluorescence using laser scanning confocal microscopy, leaf discs (Ø 7 mm) of 3-week-old St-Grx1-roGFP2 plants were pre-incubated in imaging buffer (10 mM MES pH 5.8, 10 mM $MgCl_2$, 10 mM $CaCl_2$, 5 mM KCl) for 30 min and then transferred onto a microscope slide. The samples on the slide were covered with either ddH_2O, 100 mM H_2O_2 or 100 mM DTT and mounted into the light pass of a Leica

SP8 lightning (Leica Biosystems, Germany). Images were collected using a 40x lens (HC-PL-APO-C22, Zeiss) in multi-track mode with sequential excitation by 485 nm (1% gain) and 405 nm lasers (5% gain). Emitted roGFP2 fluorescence was detected from 505 to 536 nm 10 min after the treatment started.

roGFP2 fluorescence was further measured in 96 well plates using the Tristar2 LB 942 multimode reader (Berthold, Germany). After cutting the leaf discs (Ø 7 mm) of 3-week-old St-Grx1-roGFP2 and At-Grx1-roGFP2 samples were placed into ddH_2O for 1 h to rest. For measurements the leaf discs were transferred individually into a 96-well plate containing 100 µL ddH_2O. Measurements took place with 2-minute intervals for 10 min to measure the basal level of fluorescence, followed by application of different treatments (mock, H_2O_2 or DTT) using a stock solution with 2x the final concentration and a volume equal to the starting volume (100 µL), with continuous measuring for a minimum of 70 min after treatment application. Exposure time was set manually to 0.1 s with an alternating excitation at 405 nm (30% lamp energy) and 485 nm (30% lamp energy) using a 535 ± 15 nm emission filter. Redox changes were represented as the ratio of the emission after measurements at both excitation wavelengths (405/485) at 10 min after applying the stimulus.

Statistics

All Ca^{2+} and redox measurements include data from nine individual replicates. For those nine measurements, the plants were grown independently three times and leaf discs were obtained from three independent plants each time. Pairwise comparisons were performed via students t-test with a significance threshold of $p \leq 0.01$. All data are represented as means ± SE. Details of the statistical analysis are specified in figure legends.

Data availability

The data used to support the findings of this study are included within the manuscript or supplementary information files.

Received: 8 May 2024; Accepted: 6 November 2024
Published online: 11 November 2024

References

1. Rizhsky, L. et al. When defense pathways collide. The response of Arabidopsis to a combination of drought and heat stress. *Plant Physiology* **134**, 1683–1696 (2004).
2. Takahashi, F., Kuromori, T., Urano, K., Yamaguchi-Shinozaki, K. & Shinozaki, K. Drought stress responses and resistance in plants: From cellular responses to long-distance intercellular communication. *Front. Plant Sci.* **11**, 556972 (2020).
3. Rasmussen, S. et al. Transcriptome responses to combinations of stresses in Arabidopsis. *Plant Physiology* **161**, 1783–1794 (2013).
4. Zandalinas, S. I. et al. Systemic signaling during abiotic stress combination in plants. *Proc. Natl. Acad. Sci. U.S.A.* **117**, 13810–13820 (2020).
5. Kudla, J., Batistič, O. & Hashimoto, K. Calcium signals: The lead currency of plant information processing. *Plant Cell* **22**, 541–563 (2010).
6. Pirayesh, N., Giridhar, M., Ben Khedher, A., Vothknecht, U. C. & Chigri, F. Organellar calcium signaling in plants: An update. *Biochimica et Biophysica Acta (BBA) - Molecular Cell Research* **1868**, 118–948 (2021).
7. Ghosh, S., Bheri, M., Bisht, D. & Pandey, G. K. Calcium signaling and transport machinery: Potential for development of stress tolerance in plants. *Current Plant Biology* **29**, 100235 (2022).
8. Plieth, C., Hansen, U., Knight, H. & Knight, M. R. Temperature sensing by plants: The primary characteristics of signal perception and calcium response. *The Plant Journal* **18**, 491–497 (1999).
9. Knight, H. & Knight, M. R. Imaging spatial and cellular characteristics of low temperature calcium signature after cold acclimation in Arabidopsis. *Journal of Experimental Botany* **51**, 1679–1686 (2000).
10. McAinsh, M. R. & Pittman, J. K. Shaping the calcium signature. *New Phytologist* **181**, 275–294 (2009).
11. Whalley, H. J. & Knight, M. R. Calcium signatures are decoded by plants to give specific gene responses. *New Phytologist* **197**, 690–693 (2013).
12. Knight, M. R., Campbell, A. K., Smith, S. M. & Trewavas, A. J. Transgenic plant aequorin reports the effects of touch and cold-shock and elicitors on cytoplasmic calcium. *Nature* **352**, 524–526 (1991).
13. Knight, H., Trewavas, A. J. & Knight, M. R. Calcium signalling in *Arabidopsis thaliana* responding to drought and salinity. *The Plant Journal* **12**, 1067–1078 (1997).
14. Rentel, M. C. & Knight, M. R. Oxidative stress-induced calcium signaling in Arabidopsis. *Plant Physiology* **135**, 1471–1479 (2004).
15. Jiang, Z. et al. Relationship between $NaCl^-$ and H_2O_2-induced cytosolic Ca^{2+} increases in response to stress in Arabidopsis. *PLoS ONE* **8**, e76130 (2013).
16. Thor, K. & Peiter, E. Cytosolic calcium signals elicited by the pathogen-associated molecular pattern flg22 in stomatal guard cells are of an oscillatory nature. *New Phytologist* **204**, 873–881 (2014).
17. Mithöfer, A. & Mazars, C. Aequorin-based measurements of intracellular Ca^{2+}-signatures in plant cells. *Biol Proced Online* **4**, 105–118 (2002).
18. Zhang, Y. et al. Aequorin-based luminescence imaging reveals differential calcium signalling responses to salt and reactive oxygen species in rice roots. *Journal of Experimental Botany* **66**, 2535–2545 (2015).
19. Nagel-Volkmann, J., Plieth, C., Becker, D., Lüthen, H. & Dörffling, K. Cold-induced cytosolic free calcium ion concentration changes in wheat. *Journal of Plant Physiology* **166**, 1955–1960 (2009).
20. Albert, M., Van Der Krol, S. & Kaldenhoff, R. *Cuscuta reflexa* invasion induces Ca^{2+} release in its host. *Plant Biology* **12**, 554–557 (2010).
21. Giridhar, M. et al. Comparative analysis of stress-induced calcium signals in the crop species barley and the model plant Arabidopsis thaliana. *BMC Plant Biol* **22**, 447 (2022).
22. World Food and Agriculture. *Statistical Yearbook 2021* (FAO, 2021). https://doi.org/10.4060/cb4477en.
23. Kim, Y.-U. & Lee, B.-W. Differential mechanisms of potato yield loss induced by high day and night temperatures during tuber initiation and bulking: Photosynthesis and tuber growth. *Front. Plant Sci.* **10**, 300 (2019).
24. Chinnusamy, V., Jagendorf, A. & Zhu, J. Understanding and improving salt tolerance in plants. *Crop Sci.* **45**, 437–448 (2005).
25. Moroz, N. & Tanaka, K. FlgII-28 is a major flagellin-derived defense elicitor in potato. *MPMI* **33**, 247–255 (2020).
26. Mittler, R. ROS are good. *Trends in Plant Science* **22**, 11–19 (2017).
27. Mattila, H., Khorobrykh, S., Havurinne, V. & Tyystjärvi, E. Reactive oxygen species: Reactions and detection from photosynthetic tissues. *Journal of Photochemistry and Photobiology B: Biology* **152**, 176–214 (2015).

28. Ranf, S., Eschen-Lippold, L., Pecher, P., Lee, J. & Scheel, D. Interplay between calcium signalling and early signalling elements during defence responses to microbe- or damage-associated molecular patterns. *The Plant Journal* **68**, 100–113 (2011).
29. Seybold, H. et al. Ca^{2+} signalling in plant immune response: From pattern recognition receptors to Ca^{2+} decoding mechanisms. *New Phytologist* **204**, 782–790 (2014).
30. Mithöfer, A., Ebel, J., Bhagwat, A. A., Boller, T. & Neuhaus-Url, G. Transgenic aequorin monitors cytosolic calcium transients in soybean cells challenged with β-glucan or chitin elicitors. *Planta* **207**, 566–574 (1999).
31. Maintz, J. et al. Comparative analysis of MAMP-induced calcium influx in Arabidopsis seedlings and protoplasts. *Plant and Cell Physiology* **55**, 1813–1825 (2014).
32. Marcec, M. J. & Tanaka, K. Crosstalk between calcium and ROS signaling during Flg22-triggered immune response in Arabidopsis leaves. *Plants* **11**, 14 (2021).
33. Chi, Y. et al. Flg22-induced Ca^{2+} increases undergo desensitization and resensitization. *Plant Cell & Environment* **44**, 3793–3805 (2021).
34. Rosenwasser, S. et al. A fluorometer-based method for monitoring oxidation of redox-sensitive GFP (roGFP) during development and extended dark stress. *Physiologia Plantarum* **138**, 493–502 (2010).
35. Barberini, M. L. et al. Calcium dynamics in tomato pollen tubes using the Yellow Cameleon 3.6 sensor. *Plant Reprod* **31**, 159–169 (2018).
36. Ali, A., Petrov, V., Yun, D.-J. & Gechev, T. Revisiting plant salt tolerance: Novel components of the SOS pathway. *Trends in Plant Science* **28**, 1060–1069 (2023).
37. Liang, L. et al. Genome-wide characterization of SOS1 gene family in potato (*Solanum tuberosum*) and expression analyses under salt and hormone stress. *Front. Plant Sci.* **14**, 1201730 (2023).
38. Wang, C.-F., Han, G.-L., Yang, Z.-R., Li, Y.-X. & Wang, B.-S. Plant salinity sensors: Current understanding and future directions. *Front. Plant Sci.* **13**, 859224 (2022).
39. Yuan, F. et al. OSCA1 mediates osmotic-stress-evoked Ca^{2+} increases vital for osmosensing in Arabidopsis. *Nature* **514**, 367–371 (2014).
40. Sun, S., Zhang, X., Chen, K., Zhu, X. & Zhao, Y. Screening for Arabidopsis mutants with altered Ca^{2+} signal response using aequorin-based Ca^{2+} reporter system. *STAR Protocols* **2**, 100558 (2021).
41. Zhu, X. et al. Measuring spatial and temporal Ca^{2+} signals in Arabidopsis plants. *JoVE* https://doi.org/10.3791/51945 (2014).
42. Clayton, H., Knight, M. R., Knight, H., McAinsh, M. R. & Hetherington, A. M. Dissection of the ozone-induced calcium signature. *The Plant Journal* **17**, 575–579 (1999).
43. Hipsch, M. et al. Sensing stress responses in potato with whole-plant redox imaging. *Plant Physiology* **187**, 618–631 (2021).
44. Bourke, A., Hill, J. R. & Ó Gráda, C. *The Visitation of God? The Potato and the Great Irish Famine* (Lilliput Press, 1993).
45. Nürnberger, T. et al. High affinity binding of a fungal oligopeptide elicitor to parsley plasma membranes triggers multiple defense responses. *Cell* **78**, 449–460 (1994).
46. Blume, B., Nürnberger, T., Nass, N. & Scheel, D. Receptor-mediated increase in cytoplasmic free calcium required for activation of pathogen defense in parsley. *Plant Cell* **12**, 1425–1440 (2000).
47. Davis, R. M. First report of phytophthora root rot of parsley. *Plant Dis.* **78**, 1122D (1994).
48. Stael, S. et al. Plant organellar calcium signalling: an emerging field. *Journal of Experimental Botany* **63**, 1525–1542 (2012).
49. Demidchik, V., Shabala, S., Isayenkov, S., Cuin, T. A. & Pottosin, I. Calcium transport across plant membranes: Mechanisms and functions. *New Phytol* **220**, 49–69 (2018).
50. Xu, X. et al. Genome sequence and analysis of the tuber crop potato. *Nature* **475**, 189–195 (2011).
51. Aller, I., Rouhier, N. & Meyer, A. J. Development of roGFP2-derived redox probes for measurement of the glutathione redox potential in the cytosol of severely glutathione-deficient rml1 seedlings. *Front. Plant Sci.* **4**, 66 (2013).
52. Rocha-Sosa, M. et al. Both developmental and metabolic signals activate the promoter of a class I patatin gene. *The EMBO Journal* **8**, 23–29 (1989).
53. Nietzel, T. et al. The fluorescent protein sensor ro GFP 2-Orp1 monitors *in vivo* H_2O_2 and thiol redox integration and elucidates intracellular H_2O_2 dynamics during elicitor-induced oxidative burst in Arabidopsis. *New Phytologist* **221**, 1649–1664 (2019).
54. Knight, H. & Knight, M. R. Chapter 14 recombinant aequorin methods for intracellular calcium measurement in plants. in *Methods in Cell Biology* vol. 49 201–216 (Elsevier, 1995).

Acknowledgements

We are grateful to Marc R. Knight (Durham University) for critical assessment of the manuscript. We thank the Solana Research GmbH for generation of the St-Grx1-roGFP2 lines, Stephan Hartmann, who carried out the initial screen to select GRX1-roGFP2 line #29, and Ursula Mettbach for the maintenance of all potato lines. We also thank Jose Ugalde (University of Bonn) and Sakil Mahmud (now University of Missouri) for support with the set-up of the in vivo roGFP2 imaging and Andreas Meyer (University of Bonn) for help with roGFP2 measurements. We acknowledge funding to A.B., R.E.S., S.S., U.C.V. and A.v.D by the EU Horizon 2020 research and innovation project ADAPT (GA 2020 862-858) and to U.C.V by the DFG (INST 217/939-1 FUGG).

Author contributions

A.v.D. contributed to conceptualization, investigation (responsible for most experimental work), formal analysis, validation, visualization, and writing - original draft as well as review & editing; R.E.S. and A.B. contributed to conceptualization, investigation and writing - original draft; S.S. contributed to resources (potato transformation and selection) and writing - review & editing; U.C.V. contributed to conceptualization, formal analysis, validation, funding acquisition, project administration, supervision, and writing – review & editing.

Funding

Open Access funding enabled and organized by Projekt DEAL.

Declarations

Competing interests

The authors declare no competing interests.

Ethics Declaration

All methods were carried out in accordance with Cartagena protocol domestic law and related regulations

and followed the instructions given by the providers of the plant material. *Solanum tuberosum* plants (cultivar Désirée) were used in this study. Plants expressing the apoprotein aequorin were created and kindly provided by Dr. Sophia Sonnewald (Department of Biology, Chair of Biochemistry, Friedrich-Alexander-University Erlangen-Nuremberg, Germany) and plants expressing the Grx1-roGFP2 sensor were created and kindly provided by Solana Research GmbH. *Arabidopsis* mutant lines (Col-0) carrying the apoprotein aequorin were kindly provided by Prof. Dr. Marc Knight (Department of Biosciences, Durham University, United Kingdom). *Arabidopsis* mutants expressing the Grx1-roGFP2 sensor were kindly provided by Prof. Dr. Andreas Meyer (Department of Chemical Signalling, Bonn University, Germany).

Additional information

Supplementary Information The online version contains supplementary material available at https://doi.org/10.1038/s41598-024-79134-3.

Correspondence and requests for materials should be addressed to A.D. or U.C.V.